

High-Fidelity Quantum Information Transmission using a Nonrefrigerated Lossy Microwave Waveguide at Room Temperature

Montasir Qasymeh¹ and Hichem Eleuch^{2,3}

¹*Electrical and Computer Engineering Department, Abu Dhabi University, 59911 Abu Dhabi, UAE*

²*Department of Applied Physics and Astronomy, University of Sharjah, Sharjah, United Arab Emirates*

³*Institute for Quantum Science and Engineering, Texas AM University, College Station, TX 77843 USA*

Quantum microwave transmission is key to realizing modular superconducting quantum computers [1] and distributed quantum networks [2]. However, a large number of incoherent photons are thermally generated in the microwave frequency spectrum. Hence, high fidelity quantum microwave transmission has long been believed to be infeasible without refrigeration [3, 4]. In this work, we propose a novel method for high fidelity quantum microwave transmission using a lossy waveguide at room temperature. The proposed scheme considers two cryogenic nodes (i.e., a transmitter and a receiver) connected by a room-temperature lossy microwave waveguide. First, a cryogenic pre-amplification is provided before transmission. Second, at the receiver side, a cryogenic loop antenna coupled to an *LC* harmonic oscillator inside the output port of the waveguide is implemented, while the *LC* harmonic oscillator is located outside the waveguide. The loop antenna converts the quantum microwave fields (which contain both signal and noise photons) to a quantum voltage across the coupled *LC* harmonic oscillator. The induced noise photons across the *LC* oscillator include the amplification noise, the thermal occupation of the waveguide, and the fluctuation-dissipation noise. The loop antenna detector at the receiver is designed to extensively suppress the induced noise photons across the *LC* oscillator to achieve effectively cooled waveguide. We show that by properly designing the pre-amplification gain, along with the loop antenna at the receiver, a high fidelity quantum transmission (i.e., more than 0.97) can be achieved for transmission distances reaching 100 m.

I. INTRODUCTION

Realizing large-scale quantum computers with thousands (or millions) of qubits requires efficient quantum data transmission between distant quantum nodes [5–7]. This architecture of remotely connected quantum modules is known as a modular quantum computer [8], which is believed to overcome the current challenges that prevent scaling up of quantum computers, such as crosstalk, input/output coupling limitations, and limited space [9, 10]. Likewise, future quantum sensing applications and networks require efficient quantum transmissions with applicable implementations [11–15]. Among the main quantum technologies, superconducting-based quantum circuits have shown exceptional potential for quantum signal processing and computation [16–18]. However, the superconducting signals are particularly vulnerable to thermal energy, as they operate in the microwave frequency spectrum. Therefore, superconducting circuits are typically housed in cryostats. This operation condition imposes rigorous limitations on the possibility of building modular superconducting quantum computers. Several approaches have been proposed to connect distant superconducting quantum circuits. One approach is based on entangling distant superconducting circuits using coaxial cables carrying microwave photons [19–21] or acoustic channels carrying phonons [22]. The reported transmission lengths when using this technique were between 1 and 2 m. Another approach using a cooled microwave waveguide at cryogenic temperatures was demonstrated [3]. Five metre coherent microwave transmission was reported. The above two approaches require housing the transmission channels in dilution refrigerators, which is challenging from an economic and implementation standpoint. In this regard, IBM announced plans to build a jumbo liquid-helium refrigerator 10 feet tall and 6 feet wide to support

the planned 1000 qubits quantum computer for 2023 and the milestone million qubits quantum computer lined up for 2030 [23]. In [24, 25], transmitting quantum information via noisy channels have been proposed using a time-dependant coupling between the qubits (at the transmitter and receiver) and the connecting channel. However, the channel loss and the dissipation-generated noise have not been taken into account. Also, these approaches require operating at few Kelvins (i.e., 4 K), and implementing quantum-error correction to attain high transmission fidelity. Alternatively, others proposed connecting superconducting cryogenic circuits (or processors) by utilizing optical fibers with the help of microwave-to-optical transduction [4, 26–28]. However, several challenges still remain in realizing efficient wide-band electro-optic transducers, in addition to the transduction drawbacks of adding conversion noise and laser-induced quasiparticles[3].

In this work, we propose a novel approach for transmitting coherent quantum microwave fields using a lossy room-temperature microwave waveguide. The proposed scheme includes a microwave waveguide connecting two distant superconducting circuits housed in cryostats, while the waveguide is placed outside the refrigerators and operates at room temperature, as shown in Fig. 1. The principle of operation is based on utilizing a superconducting loop antenna, coupled to an *LC* harmonic oscillator at the receiving end of the transmission waveguide. According to the principle of *Faraday's law* of induction, the loop antenna converts the microwave fields to microwave voltages across the *LC* harmonic oscillator. The induced voltages in the *LC* oscillator include both the transmitted signal and the noise photons. Interestingly, by properly designing the loop antenna dimensions, the number of induced noise photons in the *LC* harmonic oscillator can be significantly suppressed. Additionally, the signal transmittance can be maintained unity utilizing cryogenic preampli-

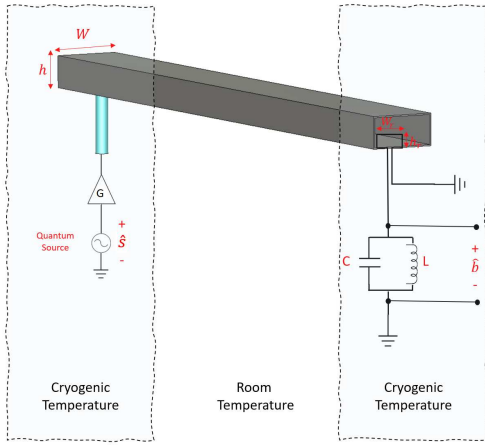


FIG. 1: Proposed microwave transmission system using a room-temperature waveguide.

fications. Consequently, we show that near-quantum limited noise temperature operation and high fidelity transmission can be achieved. Hence, the proposed scheme allows the use of a microwave waveguide operating at room temperature to connect two superconducting quantum circuits housed in distant separated cryostats. Such an approach has the potential to enable a modular superconducting quantum computer (or local quantum network) without the need for any transduction or waveguide cooling. In the remaining parts of the paper, we develop a theoretical model for the proposed scheme and provide numerical estimations considering a typical aluminium waveguide that supports the TE_{10} fundamental propagation mode.

II. RESULTS

Consider two separated superconducting quantum nodes (transmitter and receiver) placed in two distant dilution refrigerators. The two nodes are interconnected by a non-refrigerated lossy microwave waveguide. The quantum signal at the transmitter is pre-amplified at cryogenic temperature before being launched into the microwave waveguide, as shown in Fig. 1. The pre-amplifier is coupled to the microwave waveguide with unity coupling coefficient, while the latter is designed to support the fundamental TE_{10} mode. Hence, the annihilation operator of the TE_{10} mode at the input port of the waveguide is calculated by the input–output relation [29, 30], given by:

$$\hat{u} = \sqrt{G}\hat{s} + \sqrt{G}\sqrt{F_a}\hat{f}_s - \hat{f}_w, \quad (1)$$

where \hat{u} and \hat{s} are the annihilation operators of the TE_{10} mode and the source signal at the transmitter, and G and F_a are the gain and the noise-factor of the cryogenic preamplifier, respectively, \hat{f}_s is the source-generated noise operator and \hat{f}_w is the waveguide thermal noise operator. The noise operators are characterized by zero averages $\langle \hat{f}_s \rangle = \langle \hat{f}_w \rangle = 0$, and asso-

ciated noise photons give by $N_s = \langle \hat{f}_s^\dagger \hat{f}_s \rangle = \frac{1}{2} \coth(\frac{\hbar\omega}{4\pi k_b T_s})$ [34], and $N_{th} = \langle \hat{f}_w^\dagger \hat{f}_w \rangle = \frac{1}{\exp(\hbar\omega/k_B T) - 1}$. Here, T_s and T are the cryogenic source temperature and the waveguide room temperature, respectively.

The governing equation of motion of the propagating TE_{10} mode in the microwave waveguide is given by (see Methods): $\frac{\partial \hat{u}(t)}{\partial t} = -\frac{\Gamma}{2}\hat{u}(t) + \sqrt{\Gamma}\hat{f}_L(t)$, where Γ is the decay coefficient, and $\hat{f}_L(t)$ is the quantum noise operator, which obeys the relations $\langle f_L(t_1)^\dagger f_L(t_2) \rangle = N_{th}\delta(t_1 - t_2)$. The expression of the field operator $\hat{u}(t)$ at the output of the rectangular waveguide is given by:

$$\begin{aligned} \hat{u}(\tau) = & \hat{s}\sqrt{G}e^{-\frac{\Gamma}{2}\tau} + \left(\sqrt{G}\sqrt{F_a}\hat{f}_s - \hat{f}_w\right)e^{-\frac{\Gamma}{2}\tau} \\ & + \sqrt{\Gamma}e^{-\frac{\Gamma}{2}\tau} \int_0^\tau e^{\frac{\Gamma}{2}t} \hat{f}_L(t) dt, \end{aligned} \quad (2)$$

where $\tau = \frac{l}{v_g}$ is the interaction/propagation time, l is the waveguide length, and v_g is the group velocity of the TE_{10} mode. We note here that the noise operators \hat{f}_s , \hat{f}_w and \hat{f}_L are uncorrelated.

Using the solution in Eq. 2 and the noise properties, one can show that the number of photons of the TE_{10} mode at the output of the rectangular waveguide is given by:

$$\begin{aligned} \langle \hat{u}(\tau)^\dagger \hat{u}(\tau) \rangle = & \langle \hat{s}^\dagger \hat{s} \rangle Ge^{-\Gamma\tau} + \left(GF_a N_s - N_{th}\right)e^{-\Gamma\tau} \\ & + N_{th}(1 - e^{-\Gamma\tau}). \end{aligned} \quad (3)$$

Here, the first term is the number of TE_{10} signal photons, while the second and the third terms are the number of noise photons.

To suppress noise photons and achieve coherent signal transmission, we propose the following approach. A superconducting loop antenna is implemented inside the waveguide output port and subjected to the TE_{10} flux. An LC harmonic oscillator placed outside the waveguide is coupled to the loop antenna, as schematically demonstrated in Fig. 1. The loop antenna induces a voltage across the coupled LC harmonic oscillator based on Faraday's law of induction. The antenna and the LC circuit are designed to suppress the noise photons to a level obtained in case of a cooled waveguide at cryogenic temperature. The expression of the number of induced photons across the LC harmonic oscillator can be calculated using the input–output relation, and the relation (20) (see Methods), given by:

$$\begin{aligned} \langle \hat{b}^\dagger \hat{b} \rangle = & \eta G \langle \hat{s}^\dagger \hat{s} \rangle e^{-\Gamma\tau} + \eta \left(GF_a N_s - N_{th}\right)e^{-\Gamma\tau} \\ & + \eta N_{th}(1 - e^{-\Gamma\tau}) + \eta N_{th}, \end{aligned} \quad (4)$$

The first term in Eq. 4 is the number of induced signal photons (denoted M_s), while the sum of the second and third terms is the number of induced noise photons (denoted M_n). Here, $\eta = \frac{C\omega^2\mu_r^2\mu_0^2h_r^2W_r^2}{\frac{1}{2}\Omega^2lWh(\epsilon_0\epsilon_{eff}Z_F^2 + \mu_0\mu_r)}$, C is the capacitance, and W_r and h_r are the width and height of the loop antenna, respectively. We note here that the antenna dimensions are designed

to control the parameter η to properly suppress the noise photons while a cryogenic preamplification gain is provided to maintain the desired number of signal photons.

The cryogenic amplification in superconducting quantum circuits placed in dilution refrigerators is typically composed of two stages[9]. The first stage is conducted at a cryogenic temperature of a few mK using a travelling wave parametric(TWPA) amplifier. The second stage is conducted at a few K (e.g., 3 K) cryogenic temperature using a high-electron-mobility transistor (HEMT) amplifier. On considering a TWPA and HEMT amplifiers with G_T and G_H gain, and F_T and F_H noise-factor, respectively, the total amplification gain is given by $G = G_T \cdot G_H$, while the total noise-factor is given by $F_a = F_T + \frac{F_H - 1}{G_T}$. Normally, the noise-factors are expressed in term of the noise temperatures through the relation $F_j = 1 + \frac{T_j^N}{T_j^I}$. Here, $j \in \{T, H\}$ for the TWPA and HEMT amplifiers, respectively, T_j^N is the noise temperature, and T_j^I is the input noise temperature. The input noise temperature of the two amplifiers is given by $T_j^I = \frac{\hbar\omega}{4\pi k_b} \coth(\frac{\hbar\omega}{4\pi k_b T_j^O})$ [34], where T_j^O is the corresponding physical operating temperature. The noise temperature of the TWPA amplifier is given by $T_T^N = \frac{\hbar\omega}{2\pi k_b} \left(\frac{1}{G_T \ln(1 + \frac{1}{G_T - 1})} - \frac{1}{2} \right)$ [35], while the noise temperature of the HEMT amplifier is typically in the order of few Kelvins. In this work, we consider a practical TWPA amplifier of $G_T = 10$ dB gain and operating temperature of $T_T^O = 20mK$, and an off-the-shelf commercially available HEMT amplifier of $G_H = 30$ dB gain, operating temperature of $T_H^O = 10K$, and noise temperature of $T_H^N = 4.4k$ [36].

The signal transmittance and the output signal-to-noise ratio (across the LC harmonic oscillator) can be obtained from E.q. (4), given by:

$$T_r = \eta G e^{-\Gamma\tau}. \quad (5)$$

$$SNR_o = \frac{\langle \hat{s}^\dagger \hat{s} \rangle}{N_s F_a + 2 \frac{N_{th}}{G} e^{\Gamma\tau}}. \quad (6)$$

Fig. 2 (a) shows the signal transmittance versus the preamplification gain considering waveguide length of $L = 100$ m. On the other hand, the number of noise photons induced across the LC harmonic oscillator (M_n) is shown in Fig. 2 (b). As can be seen, the transmittance can be maintained close to unity by controlling (increasing) the antenna parameter η for a given gain and waveguide length. Nevertheless, at the same time, a larger number of noise photons are induced across the LC harmonic oscillator. The output signal-to-noise ratio (SNR_o) is shown in Fig. 2 (c) for the same parameters and assuming $\langle \hat{s}^\dagger \hat{s} \rangle = 40$ signal photons. Also, in Fig. 2 (d), the SNR_o and the number of induced noise photons are shown versus the waveguide length. Here, same parameters are assumed with gain of $G = 40$ dB. One can see that the SNR_o is independent of the loop antenna parameter η as both the signal photons and the induced noise photons are equally scaled by η . However, larger transmittance (for larger η) provides larger number of signal and noise photons.

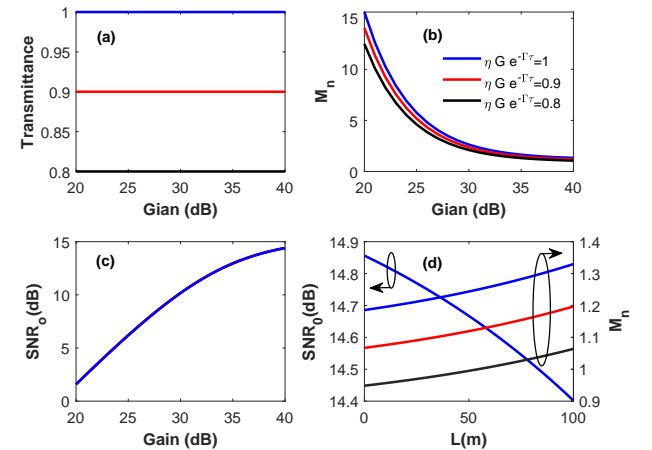


FIG. 2: (a) The signal transmittance versus gain. Here, waveguide length $L = 100$ m. (b) The number of induced noise photons (M_n) versus gain. Here, waveguide length $L = 100$ m. Different signal transmittance is considered. (c) The signal-to-noise versus gain. Here, waveguide length $L = 100$ m. (d) The signal-to-noise ratio and the number of induced noise photons (M_n) versus waveguide length. Here, the gain is $G = 40$ dB. Different signal transmittance is considered.

The performance of the transmission system can be described by calculating its noise temperature T_{Sys}^N , given by:

$$T_{Sys}^N = (F_s - 1) T_{Sys}^I, \quad (7)$$

where T_{Sys}^I is the input noise temperature of the system (which is equal to the TWPA input noise temperature T_T^I), and $F_s = \frac{SNR_I}{SNR_O} = F_a + \frac{2N_{th}}{GN_s} e^{\Gamma\tau}$ is the system noise-factor, where $SNR_I = \frac{\langle \hat{s}^\dagger \hat{s} \rangle}{N_s}$ is the input signal-to-noise ratio at the source.

Fig. 3 shows the system noise temperature (compared to the quantum-limit noise temperature) versus the waveguide length. Here, $T_Q^N = \frac{\hbar\omega}{4\pi k_b}$ is the quantum-limit noise temperature. Interestingly, by providing proper preamplification and loop antenna design at the receiver, the proposed system show a near-quantum-limited transmission. For instance, the system noise temperature is only 12 times of the quantum limit noise temperature at 10 GHz, while it is only 1.8 at 60 GHz. This is very interesting finding showing the viability of the proposed system as quantum inter-connector.

For further performance evaluation, we consider a single quantum bit information generated by the cryogenic source in Fig.1 and launched to the room-temperature waveguide for transmission through the proposed system. The generated quantum state at the source is given by[31, 32]:

$$|\psi_s\rangle = a|0\rangle + b \int_{-\infty}^{+\infty} d\omega \xi(\omega) |1_\xi\rangle + \hat{f}_s^\dagger |0\rangle, \quad (8)$$

where $|0\rangle$ and $|1_\xi\rangle$ are the vacuum and the wave-packet states, respectively, $\xi(\omega)$ is the spectral profile of the generated wave-

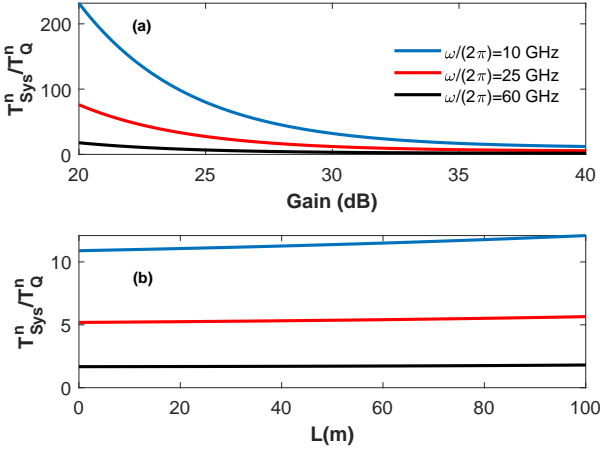


FIG. 3: (a) The normalized system noise temperature (with respect to the quantum-limit noise temperature) versus gain. Here, waveguide length $L = 100$ m, transmittance $T_r = 1$, and three different signal frequencies are considered. (b) The normalized system noise temperature (with respect to the quantum-limit noise temperature) versus waveguide length. Here, gain of $G = 40$ dB, transmittance $T_r = 1$, and three different signal frequencies are considered.

packet, and \hat{f}_s is the aforementioned source-generated thermal noise. Here, $\int_{-\infty}^{+\infty} d\omega' \int_{-\infty}^{+\infty} d\omega \xi^*(\omega') \xi(\omega) = 1$ and $\langle \hat{f}_s \rangle = 0$.

Hence, the source density matrix $\rho_s = |\psi_s\rangle\langle\psi_s|$ is given by:

$$\rho_s = |a|^2 |0\rangle\langle 0| + |b|^2 |1_\xi\rangle\langle 1_\xi| + ab^* \int_{-\infty}^{+\infty} d\omega' \xi^*(\omega') |0\rangle\langle 1_\xi| + ba^* \int_{-\infty}^{+\infty} d\omega \xi(\omega) |1_\xi\rangle\langle 0| + N_s |0\rangle\langle 0|. \quad (9)$$

Using the expression in Eq.(2), the input-output relation, and the relation in Eq.(20), the output quantum state across the LC harmonic oscillator is given by:

$$|\psi_{LC}\rangle = a\sqrt{G}\sqrt{\eta}e^{-\frac{\Gamma}{2}\tau}|0\rangle + b\sqrt{G}\sqrt{\eta}e^{-\frac{\Gamma}{2}\tau} \int_{-\infty}^{+\infty} d\omega \xi(\omega) |1_\xi\rangle + \left(\sqrt{G}\sqrt{F_a} \hat{f}_s^\dagger - \hat{f}_w^\dagger \right) \sqrt{\eta}e^{-\frac{\Gamma}{2}\tau} |0\rangle + \sqrt{\eta} \hat{f}_w^\dagger |0\rangle + \sqrt{\Gamma} \sqrt{\eta}e^{-\frac{\Gamma}{2}\tau} \left[\int_0^\tau e^{\frac{\Gamma}{2}t} \hat{f}^\dagger(t) dt \right] |0\rangle. \quad (10)$$

The first two terms in Eq. (10) are the qubit information generated by the source, the third term is the source generated noise, the fourth term is the thermal occupation noise of the waveguide, and the last term is the fluctuation-dissipation generated noise.

The output density operator $\rho_{LC} = |\psi_{LC}\rangle\langle\psi_{LC}|$ is given

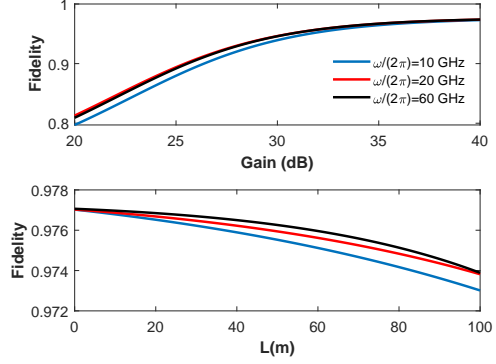


FIG. 4: (a) The transmission fidelity F versus gain. A waveguide length of $L = 100$ m and unity transmittance are considered. (b) The transmission fidelity F versus waveguide length. A gain $G = 40$ and unity transmittance are considered.

by:

$$\begin{aligned} \rho_{LC} = & |b|^2 G \eta e^{-\Gamma\tau} |1_\xi\rangle\langle 1_\xi| + |a|^2 G \eta e^{-\Gamma\tau} |0\rangle\langle 0| \\ & + ab^* G \eta e^{-\Gamma\tau} \int_{-\infty}^{+\infty} d\omega' \xi^*(\omega') |0\rangle\langle 1_\xi| \\ & + ba^* G \eta e^{-\Gamma\tau} \int_{-\infty}^{+\infty} d\omega \xi(\omega) |1_\xi\rangle\langle 0| + GF_a N_s \eta e^{-\Gamma\tau} |0\rangle\langle 0| \\ & + \eta N_{th} (1 - e^{-\frac{\Gamma}{2}\tau})^2 |0\rangle\langle 0| + \eta N_{th} (1 - e^{-\Gamma\tau}) |0\rangle\langle 0|. \end{aligned} \quad (11)$$

The closeness of the input and output quantum states in our proposed transmission systems (the pureness of the transmitted state) can be measured by calculating the fidelity F between the quantum state at the source and the quantum state across the LC harmonic oscillator at the receiver (named hereafter the transmission fidelity), given by [33]:

$$F = \frac{\text{tr}(\rho_s \rho_{LC})}{\sqrt{\text{tr}(\rho_s^2)} \sqrt{\text{tr}(\rho_{LC}^2)}}, \quad (12)$$

where $\text{tr}()$ is the trace operator.

Fig. 4 presents the transmission fidelity. Here, a unity transmittance, and three different microwave frequencies, are considered. Interestingly, a close to unity fidelity (greater than 0.97) can be attained for up to hundred metres waveguide length by providing proper preamplification. We note that in Fig. 4, the fidelity is independent of the antenna parameter η for a given gain and waveguide length. This is because while smaller η values reduce the number of the induced noise photons across the the LC harmonic oscillator, the transmittance is proportionally reduced as well, and vice versa. Therefore, we choose to consider a unity transmittance in the simulation of Fig. 4.

III. DISCUSSION

In quantum microwave transmission systems, the transmission fidelity severely degrades at room temperature due to sig-

nificant thermal occupation at such a spectrum. Towards resolving this challenge, waveguides cooling at cryogenic temperatures have been proposed to mitigate the thermal occupation and achieve an acceptable transmission quality. Other techniques such as implementing controllable coupling between the qubits (at the two side of the link) and the connecting channel have also been proposed. Potentials and limitations of these techniques were briefly discussed in the introduction above.

In this work, we proposed a novel technique to achieve an effectively cooled waveguide simply by designing proper loop antenna at the receiver side by which the induced thermal noise photons are significantly suppressed. For example, in Fig 4, the thermal waveguide occupation at room temperature is $n_{th} = 609$ for $\frac{\omega}{2\pi} = 10$ GHz microwave frequency. However, the corresponding induced noise photons across the LC harmonic oscillator is $\eta_{th} = 0.13$, which is equivalent to the same waveguide cooled at 0.255 K temperature. It is shown that a high transmission fidelity (above 0.97) can be achieved by implementing such loop antenna technique combined with proper cryogenic preamplification using a lossy room-temperature waveguide over significant transmission distances (reaching 100 m). As far we know, this is the first time a high fidelity microwave transmission system is proposed using a typical lossy non-refrigerated waveguide. Our approach has the potential to realize a modular quantum computer using waveguides placed outside the dilution refrigerators. This is very important as scaling quantum computers to the capacity of thousands of qubits crucial to leveraging quantum supremacy. While the state-of-the-art capacity of current superconducting quantum computers is less than 100 qubits [17, 23, 37], boosting the number of qubits to thousands is very challenging, especially from a heat management standpoint. This is because adding a qubit requires connecting a considerable number of cables and related components, which imposes an overwhelming heating load. For example, the cost per qubit is estimated to be approximately \$10 K to maintain the required cryogenic refrigeration while handling the pertinent cable connections[38]. Thus, the cost of a scaled quantum computer that utilizes a giant dilution refrigerator is expected to be tens of billions of dollars [39]. Connecting separated quantum nodes (or processors) by coherent signalling is a promising approach for efficient scaled quantum computation. The findings reported here have the potential to expedite realization of sought-after future modular superconducting quantum computers with the potential for thousands (million) of qubits. Finally, we note that the proposed scheme (cryogenic preamplification at the transmitter and a passive cryogenic detection circuit at the receiver) is technically very easy to implement.

IV. METHODS

Consider a microwave waveguide with rectangular cross-sectional geometry of width W along the x -axis and height h along the y -axis. The expression of the electric and magnetic fields associated with the fundamental TE_{10} mode of

this waveguide are given by [42]:

$$\vec{E}(x, y, x, t) = iAZ_F\Omega \sin\left(\frac{\pi x}{W}\right) e^{(i\beta z - \omega t)} \vec{e}_y + c.c., \quad (13)$$

$$\begin{aligned} \vec{H}(x, y, z, t) = & -iA\sqrt{\Omega^2 - 1} \sin\left(\frac{\pi x}{W}\right) e^{(i\beta z - \omega t)} \vec{e}_x \\ & + A\sqrt{\Omega^2 - 1} \sin\left(\frac{\pi x}{W}\right) e^{(i\beta z - \omega t)} \vec{e}_z + c.c., \end{aligned} \quad (14)$$

where A is the complex amplitude of the TE_{10} mode, $Z_F = 377\sqrt{\frac{\mu_r}{\epsilon_r}}$ is the impedance of the filling material, and $\Omega = \frac{\omega}{\omega_c}$. Here, ω is the microwave signal frequency, $\omega_c = \frac{2\pi c}{2W\sqrt{\epsilon_r}}$ is the cut-off frequency, μ_r and ϵ_r are the relative permeability and permittivity of the filling material, respectively, β is the propagation constant, and c is the speed of light in vacuum. In this work, we consider Aluminium waveguide (of conductivity $\sigma = 3.5 \times 10^7 S/m$) with rectangular cross-sectional area of $W = 5$ cm width and $h = 2.5$ cm height.

A. Field Quantization

The classical Hamiltonian of the TE_{10} mode is given by $\mathcal{H} = \frac{1}{2}\epsilon_0\epsilon_{eff} |A|^2 Z_F^2 \Omega^2 V_{ol} + \frac{1}{2}\mu_0\mu_r |A|^2 \Omega^2 V_{ol}$, where $V_{ol} = W \times h \times l$ is the waveguide volume and l is the waveguide length. The propagating microwave field can be quantized through the following relation:

$$A = \frac{(\hbar\omega)^{\frac{1}{2}}}{\varphi^{\frac{1}{2}}(\epsilon_0\epsilon_{eff}V_{ol})^{\frac{1}{2}}} \hat{a}, \quad (15)$$

where \hat{a} is the annihilation operator of the TE_{10} mode, $\varphi = \frac{\Omega^2 Z_F^2}{2} + \frac{\mu_0\mu_r\Omega^2}{2\epsilon_0\epsilon_{eff}}$, and $\epsilon_{eff} = \epsilon_r - \frac{\pi^2 c^2}{W^2 \omega^2}$ is the effective permittivity of the waveguide. Thus, the quantum Hamiltonian is given by $\hat{\mathcal{H}} = \hbar\omega\hat{a}^\dagger\hat{a}$. The equation of motion can be found by substituting the quantum Hamiltonian into the Heisenberg equation $\frac{\partial\hat{a}}{\partial t} = \frac{i}{\hbar}[\hat{\mathcal{H}}, \hat{a}]$. It then follows that by including the waveguide dissipation, and the dissipation-fluctuation noise, one obtains $\frac{\partial\hat{a}}{\partial t} = -i\omega\hat{a} - \frac{\Gamma}{2}\hat{a} + \sqrt{\Gamma}\hat{f}_L$. Upon implementation of a rotation approximation by setting $\hat{a} = \hat{u}e^{(-i\omega t)}$, the equation of motion reads:

$$\frac{\partial\hat{u}}{\partial t} = -\frac{\Gamma}{2}\hat{u} + \sqrt{\Gamma}\hat{f}_L, \quad (16)$$

where $\Gamma = \frac{\alpha}{v_g}$ is the decay time coefficient, $\alpha = \frac{2R_s}{\sqrt{\mu_0\mu_r}} \frac{\frac{h}{W}(\frac{\omega_r}{\omega})^2 - 1}{\sqrt{1 - (\frac{\omega_r}{\omega})^2}}$ is the attenuation coefficient, $v_g = c\sqrt{1 - (\frac{\omega_r}{\omega})^2}$ is the group velocity, and \hat{f}_L is the quantum Langevin noise operator. Here, R_s is the surface impedance of the waveguide metal material.

B. Induced Voltage

A superconducting loop antenna of width W_r along the x -axis and height h_r along the y -axis is implemented at the output port of the waveguide and is subjected to the TE_{10} flux.

The loop antenna (e.g., using NbTi wire) is coupled to an *LC* harmonic oscillator. Classically, the induced voltage across the *LC* circuit can be described by Faraday's law of induction, given by:

$$V(t) = -\frac{d\Psi}{dt}, \quad (17)$$

where $\Psi = \mu_0 \mu_r \int_0^{W_r} \int_0^{h_r} \vec{H}(x, y, z, t) \cdot d\vec{A}$ is the flux the loop antenna is subjected to and $d\vec{A} = dx dy \vec{e}_z$ is the differential element of the enclosed area of the antenna. Thus, the induced voltage across the *LC* circuit is given by $V(t) = V_I e^{-i\omega t + i\beta L} + c.c.$, where V_I is the amplitude of the induced voltage given by:

$$V_I = i\mu_0 \mu_r A h_r W_r. \quad (18)$$

The voltage across the *LC* circuit can be quantized through the following relation:

$$V_I = \sqrt{\frac{\hbar\omega}{C}} \hat{b}, \quad (19)$$

- [1] S. Daiss and S. Langenfeld and S. Welte and E. Distante and P. Thomas and L. Hartung and O. Morin and G. Rempe "A quantum-logic gate between distant quantum-network modules," *Science*, **371**, 6529 (2021).
- [2] Y. Zhong and HS. Chang and A. Bienfait and E. Dumur and M.-H. Chou and C.R. Conner and J. Grebel and R. G. Povey and H. Yan and D. I. Schuster and and A. N. Cleland "Deterministic multi-qubit entanglement in a quantum network," *Nature* **590**, 571 (2021).
- [3] P. Magnard and S. Storz and P. Kurpiers and J. Schär and F. Marxer and J. Lütolf and T. Walter and J.-C. Besse and M. Gabureac and K. Reuer and A. Akin and B. Royer and A. Blais and A. Wallraff "Microwave Quantum Link between Superconducting Circuits Housed in Spatially Separated Cryogenic Systems," *Phys. Rev. Lett.* **125**, 260502 (2020).
- [4] G. Bartholomew and J. Rochman and T. Xie and J. M. Kindem and A. Ruskuc and I. Craicu and M. Lei and A. Faraon "On-chip coherent microwave-to-optical transduction mediated by ytterbium in YVO₄," *Nat. Commun.* **11**, 3266 (2020).
- [5] D. Gottesman and I. Chuang "Demonstrating the viability of universal quantum computation using teleportation and single-qubit operations," *Nature* **402**, 390–393 (1999).
- [6] T. Northup and R. Blatt "Quantum information transfer using photons," *Nat. Photon.* **8**, 356–363 (2014).
- [7] L. Jiang and J. Taylor and A. Sørensen and M. Lukin "Distributed quantum computation based on small quantum registers," *Phys. Rev. A* **76**, 062323 (2007).
- [8] C. Monroe and R. Raussendorf and A. Ruthven and K. R. Brown and P. Maunz and L.-M. Duan and J. Kim "Large-scale modular quantum-computer architecture with atomic memory and photonic interconnects," *Phys. Rev. A* **89**, 022317 (2014).
- [9] S. Krinner and S. Storz and P. Kurpiers and P. Magnard and J. Heinsoo and R. Keller and J. Lütolf and C. Eichler and A. Wallraff "Engineering cryogenic setups for 100-qubit scale superconducting circuit systems," *EPJ Quantum Technol.* **6**, 6 (2019).
- [10] T. D. Ladd and F. Jelezko and R. Laflamme and Y. Nakamura

where \hat{b} is the annihilation operator of the voltage in the *LC* harmonic oscillator, C is the capacitance, satisfying $\omega = \frac{1}{\sqrt{LC}}$, and L is the inductance. By using the quantization relations in Eq. (15) and Eq. (19), a direct relation between the annihilation operators of the *TE*₁₀ mode and the *LC* voltage can be established, given by:

$$\hat{b} = i\hat{a} \frac{C^{\frac{1}{2}}}{\varphi^{\frac{1}{2}} (\epsilon_0 \epsilon_{eff} V_{ol})^{\frac{1}{2}}} \mu_0 \mu_r \omega h_r W_r. \quad (20)$$

where $\hat{a} = \hat{u} e^{-i\omega t}$.

Acknowledgments

This research is supported by the ASPIRE Award for Research Excellence under the Advanced Technology Research Council – ASPIRE.

and C. Monroe and J. O'Brien "Quantum computers," *Nature* **464**, 45–53 (2010).

- [11] D. Awschalom and K. Berggren and H. Bernien and S. Bhave and L. Carr and P. Davids and S. Economou and D. Englund and A. Faraon and M. Fejer and S. Guha and M. Gustafsson and E. Hu and L. Jiang and J. Kim and B. Korzh and P. Kumar and P. Kwiat and M. Loncar and M. Lukin and D. Miller and C. Monroe and S. Nam and P. Narang and J. Orcutt and M. Raymer and A. Safavi-Naeini and M. Spiropulu and K. Srinivasan, S. Sun and J. Vuckovic and E. Waks and R. Walsworth and A. Weiner and Z. Zhang "Development of quantum interconnects (QuICs) for next-generation information technologies," *PRX Quantum* **2**, 017002 (2021).
- [12] H. J. Kimble "The quantum internet," *Nature* **453**, 1023–1030 (2008).
- [13] S. Wehner and D. Elkouss and Ronald Hanson "Quantum internet: A vision for the road ahead," *Science* **362**, 6412 (2018).
- [14] L. Stephenson and D. Nadlinger and B. Nichol and S. An and P. Drmota and T. Ballance and K. Thirumalai and J. Goodwin and D. Lucas and C. Ballance "High-Rate, High-Fidelity Entanglement of Qubits Across an Elementary Quantum Network," *LPhys. Rev. Lett.* **124**, 110501 (2019).
- [15] Z. Zhang and S. Mouradian and F. Wong and J. Shapiro "Entanglement-Enhanced Sensing in a Lossy and Noisy Environment," *Phys. Rev. Lett.* **114**, 110506 (2015).
- [16] J. Mooij and T. Orlando and L. Levitov and L. Tian and C. van der Wal and S. Lloyd "Josephson Persistent-Current Qubit," *Science* **285**, 1036–1039 (1999).
- [17] F. Arute and K. Arya and R. Babbush and et al. "Quantum supremacy using a programmable superconducting processor," *Nature* **574**, 505–510 (2019).
- [18] M. Qasymeh and H. Eleuch "Hybrid two-mode squeezing of microwave and optical fields using optically pumped graphene layers," *Sci. Rep.* **10**, 16676 (2020).
- [19] C. Axline and L. Burkhardt and W. Pfaff and M. Zhang and K. Chou and P. Campagne-Ibarcq and P. Reinhold and L. Frunzio

and S. Girvin and L. Jiang and M. Devoret and R. Schoelkopf “On-demand quantum state transfer and entanglement between remote microwave cavity memories,” *Nat. Phys.* **14**, 705–710 (2018).

[20] P. Kurpiers and P. Magnard and T. Walter and B. Royer and M. Pechal and J. Heinsoo and Y. Salathé and A. Akin and S. Storz and J.-C. Besse and S. Gasparinetti and A. Blais and A. Wallraff “eterministic quantum state transfer and remote entanglement using microwave photons,” *Nature* **558**, 264–267 (2018).

[21] Y. Zhong and H. Chang and A. Bienfait and É. Dumur and M. Chou and C. Conner and J. Grebel and R. Povey and H. Yan and D. Schuster and A. Cleland “eterministic multi-qubit entanglement in a quantum network,” *Nature* **590**, 571–575 (2021).

[22] A. Bienfait and P. Satzinger and P. Zhong and H.-S. Chang and M.-H. Chou and C. R. Conner and É. Dumur and J. Grebel and G. A. Peairs and R. G. Povey and A. N. Cleland “Phonon-mediated quantum state transfer and remote qubit entanglement,” *Science* **364**, 368–371 (2019).

[23] J. Gambetta “IBM’s Roadmap For Scaling Quantum Technology,” IBM Research Blog , (2020).

[24] B. Vermersch and P.-O. Guimond and P. Zoller “Quantum state transfer via noisy Photonic and phononic waveguides,” *Phys. Rev. Lett.* **118**, 133601 (2017).

[25] Z.-L. Xiang and M. Zhang and L. Jiang and P. Rabl “Intracity quantum communication via thermal microwave networks,” *Phys. Rev. X* **7**, 011035 (2017).

[26] M. Qasymeh and H. Eleuch “Quantum microwave-to-optical conversion in electrically driven multilayer graphene,” *Opt. Express* **27**, 5945–5960 (2019).

[27] M. Qasymeh and H. Eleuch “Frequency-Tunable quantum microwave to optical conversion system,” U.S. Patent 10,824,048 B2 (2020).

[28] M. Mirhosseini and A. Sipahigil and M. Kalaee and O. Painter “Superconducting qubit to optical photon transduction,” *Nature* **588**, 599–603 (2020).

[29] M. Qasymeh and H. Eleuch “Hybrid two-mode squeezing of microwave and optical fields using optically pumped graphene layers,” *Sci. Rep.* **10**, 16676 (2020).

[30] C. W. Gardiner and M. J. Collett “Input and output in damped quantum systems: Quantum stochastic differential equations and the master equation,” *Phys. Rev. A* **31**, 3761–3774 (1985).

[31] C. Lee, M. Tame, J. Lim, and J. Lee “Quantum plasmonics with a metal nanoparticle array,” *Phys. Rev. A* **85**, 063823 (2013).

[32] Z. Y. Ou “emporal distinguishability of an N-photon state and its characterization by quantum interference,” *Phys. Rev. A* **74**, 063808 (2006).

[33] X. Wang and C.-S. Yu and X.X. Yi “An alternative quantum fidelity for mized states of qudits,” *Phys. Lett. A* **373**, 58–60 (2008).

[34] S. Simbierowicz1 and V. Vesterinen and J. Milem and A. Lintunen and M. Oksanen and L. Roschier and L. Grönberg and J. Hassel and D. Gunnarsson and R. E. Lake “Characterizing cryogenic amplifiers with a matched temperature-variable,” *Review of Scientific Instruments* **92**, 034708 (2021).

[35] L. Fasolo and P. Caricato and I. Carusotto and W. Chung and A. Cian and D. Di Gioacchino and E. Enrico and P. Falferi and M. Faverzani and E. Ferri and G. Filatrella and C. Gatti and A. Giachero and D. Giubertoni and A. Greco and C. Kutlu and A. Leo and C. Ligi and P. Livreri and G. Maccarrone and B. Margesin and G. Maruccio and A. Matlashov and C. Mauro and R. Mezzena and A. G. Monteduro and A. Nucciotti and L. Oberto and S. Pagano and V. Pierro and L. Piersanti and M. Rajteri and A. Rettaroli and S. Rizzato and Y. K. Semertzidis and U. Uchaikin and A. Vinante “Bimodal Approach for Noise Figures of Merit Evaluation in Quantum-Limited Josephson Traveling Wave Parametric Amplifiers,” arXiv:2109.14924v1 , (2021).

[36] F. Heinz and F. Thome and A. Leuther and O. Ambacher “A 50-nm Gate-Length Metamorphic HEMT Technology Optimized for Cryogenic Ultra-Low-Noise Operation,” *IEEE Transactions on Microwave Theory and Techniques* **69**, 3896–3907 (2021).

[37] M. Gong and S. WANG and C. ZHA and M.-C. CHEN and H.-L. HUANG and Y. WU and Q. ZHU and Y. ZHAO and S . LI and S. GUO and H. QIAN and Y. YE and F. CHEN and C. YING and J. YU and D. FAN and D. WU and H. SU and H. DENG and H. RONG and K. ZHANG and S. CAO and J. LIN and Y. XU and L. SUN and C. GUO and N. LI and F. LIANG and V. M. BASTIDAS and K. NEMOTO and W. J. MUNRO and Y.-H. HUO and C.-Y. LU and C.-Z PENG and X. ZHU, J.-W PAN “Quantum walks on a programmable two-dimensional 62-qubit superconducting processor,” *Science* **372**, 948–952 (2021).

[38] G. Lichfield “inside the race to build the best quantum computer on Earth,” *MIT Technology Review* , (2021).

[39] J. Levy “1 million qubit quantum computers: moving beyond the current “brute force” strategy,” *SEEQC* (2020).

[40] C. Macklin and K. O’Brien and D. Hover and M. Schwartz and V. Bolkhovsky and X. Zhang and W. Oliver and I. Siddiqi “A near quantum-limited Josephson traveling-wave parametric amplifier,” *Science* **350**, 307–310 (2015).

[41] U. Mendes and S. Jezouin and P. Joyez and B. Reulet and A. Blais and F. Portier and C. Mora and C. Altimiras “Parametric amplification and squeezing with an ac- and dc-voltage biased superconducting junction,” *Phys. Rev. Applied* **11**, 034035 (2019).

[42] D. M. Pozar ‘Microwave Engineering,’ John Wiley and Sons, New York (2012).